

The dynamic fracture energy of concrete. Review of test methods and data comparison.

J. Weerheijm & I. Vegt

Delft University of Technology, The Netherlands and TNO Defence Security and Safety, Rijswijk, The Netherlands

ABSTRACT: Data on the dynamic fracture energy of concrete are scarce and also not consistent due to different test methods, data analyses and definitions. This paper intends to facilitate the discussion on dynamic fracture energy and start the standardization process for dynamic tensile testing. The response and failure mechanisms in statics and dynamics are addressed. Definitions of the fracture process zone, the fracture zone and the fracture energy are recalled. Test methods to derive strength and, especially fracture energy data for concrete in tension are summarized and reviewed. For dynamics, the uniaxial set-ups are the most suitable. To illustrate the dependency of G_f data to the applied diagnostics and data analysis, a comparison of two data sets for loading rates in the order of 1000 GPa/s is given. The paper ends with an overview of recommended test methods for uniaxial dynamic tensile testing.

1 INTRODUCTION

The response of concrete up to complete failure in tension is represented in the load-deformation relation. The characteristic parameters are the ultimate strength, stiffness in the ascending branch and the fracture energy. All these properties are rate dependent. The observed response of concrete at macro level is determined by the damage initiation and damage accumulation mechanisms at meso and micro scale level. The failure process is governed by (i) the stress condition, (ii) the ability to absorb energy in fracture and (iii) the energy flow from the surrounding material into the fracture zone. In dynamics all three conditions vary in time and depend on the loading rate. Especially at loading rates beyond 50 GPa/s these mechanisms are strongly rate dependent resulting in an extensive strength increase.

In collaboration with TNO Defence Security and Safety (TNO DSS), the Delft University of Technology (DUT) studies the dynamic response of concrete under tensile loading. The research comprises experimental and computational studies.

The focus of this paper is on the fracture energy and especially on the possibilities to quantify the fracture energy experimentally in dynamic tensile tests. First, the fracture energy will be discussed and defined theoretically. Next, the material conditions for deformation controlled static testing and dynamic testing are addressed and the applied test methods are reviewed.

The authors developed a test and measurement technique for the Split Hopkinson Bar (SHB) and, for

high loading rates, a modified Split Hopkinson Bar (MSHB) to quantify the stress - and deformation conditions independently as a function of time. Combined, these result in a load-deformation curve from which the fracture energy is obtained. The experimental results will be discussed and compared with available data from literature. Finally, specific test methods are recommended.

2 FRACTURE ENERGY STATIC CONDITIONS

The concrete response in tension up to failure is studied and described extensively in literature (e.g. Bazant, Carpinteri, Wittmann, Hillerborg, Reinhardt, van Mier). In this section a summary of the main characteristics is given as a reference for the dynamic response.

The response of concrete up to failure is governed by its heterogeneous composition and dominated by the extension of initially existing damage. Being aware of the supporting subscale material structure, the mechanical response of concrete is mainly dominated by the response at meso-scale which is characterized by aggregates, mortar matrix, the ITZ (interface transition zone) and the pores and flaws.

Due to the differences in stiffness of the various components and the induced stresses during the hardening process, the internal stress distribution is not equally distributed and initial microcracks and defects exist.

When the material strength is locally exceeded, damage will start to grow. Available deformation en-

ergy flows into the fracture zone and is absorbed in the fracture process. Because of the coarse heterogeneity the fracture does not consist of the formation of a single crack. The macrocrack is preceded by a zone in which multiple microcracking occurs. This zone is called the fracture process zone (FPZ). First the micro cracks start to grow, interfering with each other, with defects and aggregates. After a while a dominant macro crack is formed, which grows. This process is well represented in the fictitious fracture model of Hillerborg (Hillerborg 1976, 1985), see

equals the surface below the load-deformation curve for uniaxial tensile loading.

3 STATIC FRACTURE ENERGY TESTS

3.1 Direct uniaxial tension

To determine the Mode I fracture energy directly, the uniaxial tensile test is the most fundamental one. But the test is not easy to perform, special equipment is needed and discussions on the boundary conditions and the minimum specimen size to be applied, are still ongoing (van Mier 2002). The tests have to be deformation controlled also during the failure process. This results into requirements on the length of the specimen, the test equipment and diagnostics. E.g., the clamping conditions, fully rotating or non-rotating platens, will affect the recorded load-deformation curve and thus the “recorded” G_f -value. In spite of the unfinished discussions on the “ideal test”, the direct tension test is recommended to determine the uniaxial properties of concrete if the equipment is available.

3.2 Three point bending test

Because the special equipment for uniaxial testing is not commonly available, a special procedure has been developed to derive the fracture energy from the load-deflection curve measured in a three point bending test. The need for a practical method initiated a major flow of research on concrete fracture mechanics and size effects in the ‘80’s and 90’s. A standard RILEM bending-test has been developed to determine the fracture energy. G_f is defined by the recorded load-displacement relation corrected by the absorbed energy due to the dead-weight (Hillerborg 1985). In order to derive the material property G_f , from this structural test, two important “energy related” test conditions have to be fulfilled. These are: (i) the absorbed energy outside the Mode I failure zone should be ignorable and (ii) the compressive strength should be much larger than the tensile strength, else too much energy is absorbed in the compressive zone and no representative G_f value can be obtained. In the 90’s Elices, Guinea and Planas analyzed the bending test thoroughly and quantified the most important error sources and proposed an analysis procedure to deal with weight compensation and the energy dissipation at the end of the deformation tail.

For dynamic testing, the main lesson learned from all the research and publications on how to determine the fracture energy from 3-point bending tests is that the stress distribution and the energy dissipation in the whole specimen during the whole load-cycle have to be known.

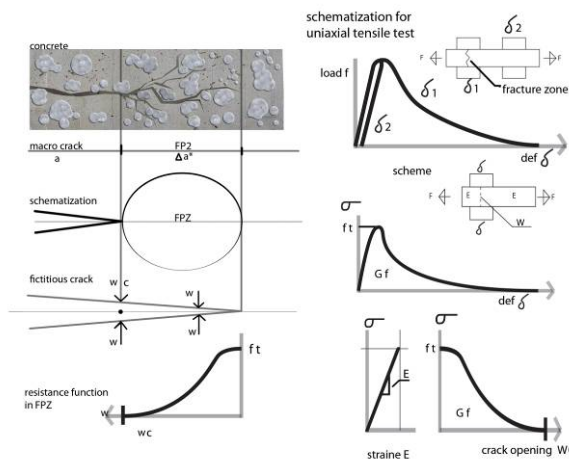


Figure 1. Crack tip fracture process; fictitious crack concept.

The approach is quite similar to the energy balance approach in which a certain amount of energy is absorbed by the formation of a unit area of crack surface. When a crack propagates, a certain amount of (deformation) energy is released. Crack propagation is controlled by the balance of released and absorbed energy (the energy criterion). In the fictitious crack model the crack initiation is controlled by the strength criterion, the maximum material strength, f_t .

To help the discussion and description of the Mode I fracture process we recall and suggest the following definitions:

- The Fracture Process Zone (FPZ) is the zone ahead of the tip of a physical, macrocrack. Microcracking in the FPZ leads to the growth of the macro crack. The FPZ is coupled to the material characteristics at meso- and microlevel.
- The Fracture Zone (FZ) covers the material that is involved in the energy exchange of the fracture process. In this zone the final failure crack is formed by the branching and coalescence of individual macrocracks (see Fig. 1 for the uniaxial tensile test). The zone includes the FPZ of these macrocracks plus the surrounding material from which deformation energy is released into crack formation.
- The material fracture energy G_f is the energy absorbed within a single fracture zone and

4 DYNAMIC CONDITIONS

4.1 *Dynamic response*

Concrete is probably the most rate dependent structural material. Especially in tension concrete exhibits a pronounced increase in strength for loading rates exceeding 15 GPa/s (corresponds to strain rate in the order of 1/s). For concrete, one can distinguish two regions for rate dependency. For loading rates ranging from static (10^{-4} GPa/s) to intermediate rate of 50 GPa/s, a moderate rate effect in tensile strength is observed. Beyond the rate of 50 GPa/s a very steep strength increase occurs. The rate effects occur due to the additional resistance to damage growth at micro- and meso level. The main mechanisms can be summarized as follows. In the moderate loading regime the moisture in the capillary pores causes the dominant effect. The water adds resistance to pore-widening (Stephan effect) under dynamic loading, which results in the observed strength increase (see e.g. Vegt et al. 2009). With increasing loading rate the inertia effects at micro level become dominant. Inertia affects the stress fields in the heterogeneous material, around the material defects and the (micro) cracks. Stress singularities decrease and damage initiation and growth are delayed. These micro inertia effects cause the pronounced strength increase beyond 15-50 GPa/s.

Ignoring the pre-peak non-linearity and damage initiation at micro level, it is stated that the main fracture and failure process starts when maximum strength is reached. Comparing the processes in statics and dynamics, the ruling mechanism is basically the same, i.e. the energy balance between the released deformation energy that flows into the fracture zone and is absorbed in the fracture process. In dynamics a part of the available energy is temporarily stored into kinetic energy. The key difference is the factor time. For the purpose of this paper, the authors want to focus on this aspect and the consequences for the definition and determination of the fracture energy.

Time governs the size of the fracture zone (FZ) as defined previously. The FZ contains the material that is involved in the energy exchange process. The width of FZ is determined by the duration of the fracture process (t_{frac}) and the longitudinal wave velocity (c_p) at which energy can be transferred into the fracture process. The width of FZ (l_{FZ}), and the intermediate distance between two final macro cracks is given by

$$l_{\text{FZ}} = 2 \cdot c_p \cdot t_{\text{frac}}$$

The wave velocity in concrete is in the order of 3500 m/s, while the duration of the fracture process is governed by the velocity of crack growth of the

micro cracks and the coalescence into the final macro crack. Besides the internal (dynamic) stress distribution, the meso structure and the number and distribution of the initial defects will determine t_{frac} . To estimate the order of magnitude of l_{FZ} , it is assumed that the dominant defects are coupled to the aggregates (e.g. diameter 8 mm), the maximum crack velocity is in the order of 500 m/s (see Weerheijm 1992), so the failure time is about 8 μsec and l_{FZ} is about 55 mm. At higher loading rates more defects in a wider zone can be activated which will result in more energy absorption, a delay of coalescence, a longer t_{frac} and consequently a larger FZ.

To understand the mechanisms of dynamic fracture, it is recommended to gain also information on t_{frac} and the crack patterns from dynamic testing.

In analogue with static testing, possibilities of the drop weight test and the uniaxial Split Hopkinson bar tests to quantify G_f will be discussed in the next sections. The lessons learned from static testing are:

- The fracture energy should be related to a single fracture zone;
- The energy (re)distribution in the specimen during testing up to failure has to be known and unique.
- In a fracture energy test, energy absorption should occur in only one zone, i.e. the fracture zone.

4.2 *Drop weight bending test*

Referring to the difficulties to derive G_f -values under static conditions, it is obvious that it will be hardly impossible to fulfill the mentioned test requirements in dynamic impact bending tests. Due to the impact event, stress waves are induced in the specimen. These waves interfere and a “stationary stress field” only occurs after a certain period after which the specimen responds in its first (quasi static) mode. Consequently, the method should be restricted to relatively low loading rates. It should also be noted that the true relation between the induced and absorbed energy in the failure zone is hard to derive from the test because of the time delay.

In spite of the limitations the impact test is used (e.g. Zhang et al. 2009) because it is, just like the static bending test, easy to perform. The main developers of the G_f -impact test are Banthia and Mindess (1987). The procedure they developed, is the following, see also Figure 2.

- The impact hammer is instrumented to record the load as a function of time, $P(t)$;
- The beam is instrumented with accelerometers to record the deformation of the beam as a function of time.
- A quasi static failure mode is assumed with a “failure hinge” in the notch section. The response is split into a dynamic inertia term and

a static bending term. The load $P(t)$ is subdivided into:

$$P(t) = P_i(t) + P_b(t)$$

- Tests show that the deformation mode can be re-presented by a linear shape for plane concrete and a sinusoidal shape for reinforced concrete. For a plane concrete beam with cross section A , $P_b(t)$ is quantified by using the recorded hammer load $P(t)$ and the mid span acceleration, $a_0(t)$, according to:

$$P_b(t) = P_i(t) - A \cdot \rho \cdot a_0(t) \cdot \left[\frac{l}{3} + \frac{8 \cdot b^3}{3 \cdot l} \right]$$

- The work performed by the “static load contribution” $P_b(t)$ equals the bending energy which is defined as the (dynamic) fracture energy of the concrete beam.

$$G_f = E_b(t) = \int_0^l P_b(t) \cdot du_0$$

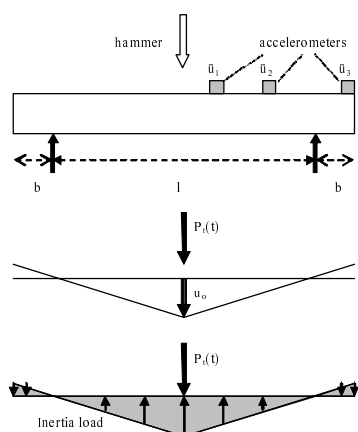


Figure 2. Scheme drop weight impact test and analysis.

Reviewing this analysis it is concluded that it is a quasi-static approach. Loading $P_b(t)$ is synchronized with midspan deflection $u_0(t)$ and complete fracture occurs when $P_b(t)$ is reduced to zero. Consequently, the constraints of the static 3-point bending tests to determine G_f , count also for the drop weight test. On top of that, it is assumed that all deformation energy is released into the fracture zone. This only counts when the specimen is stress free at the moment of complete fracture. Because of these assumptions, this method will lead to an overestimation of G_f and can not be applied for the high loading rate regimes. Because of the limitations, the authors advice against the drop weight test to determine G_f values.

4.3 Uniaxial dynamic testing.

The split Hopkinson bar technique is commonly used to determine the dynamic tensile strength in the loading rate regime 10 – 100 GPa/s. For higher loading rates the Hopkinson/Kolsky spalling bar technique is recently used by TNO/TU-Delft, EMI and the University of Metz. Because the Hopkinson bar offers a uniaxial loading condition and the energy distribution in the system can be recorded, the set-up offers also the possibility to quantify the dynamic fracture energy. In the next sections the techniques will be presented and discussed.

4.3.1 Split Hopkinson Bar, TU-Delft.

In the 1980's Reinhardt and co-workers developed a gravity driven Split Hopkinson bar for the regime of 10 -50 GPa/s. Specimen height and diameter are 100 and 75 mm respectively. The research was focused on the tensile strength. Zielinski reported also some G_f values he derived from the recorded stresses and the deformation of the whole specimen. He concluded that the rate effect on fracture energy is of the same order as the rate effect on tensile strength. Because multiple fracture occurred, see section 4.1, the total fracture energy of multiple fracture zones was quantified and not the G_f value of a single fracture zone. Weerheijm and Reinhardt applied notched, instrumented specimen to reconstruct the dynamic load-deformation curve for a single fracture zone. The deformation of the fracture zone is derived from the total deformation of the specimen minus the elastic deformation outside this zone. The stress-deformation curve is obtained by synchronizing the stress signal in the upper bar and the fracture zone deformation. G_f is given by the surface of this curve in analogue with fictitious crack model of Hillerborg for statics, see Figure 3. For the moderate loading rate regime the rate effect on G_f for the single fracture zone proves to be much lower than on the tensile strength. Quantitative results are given in Vegt 2009 and section 5.

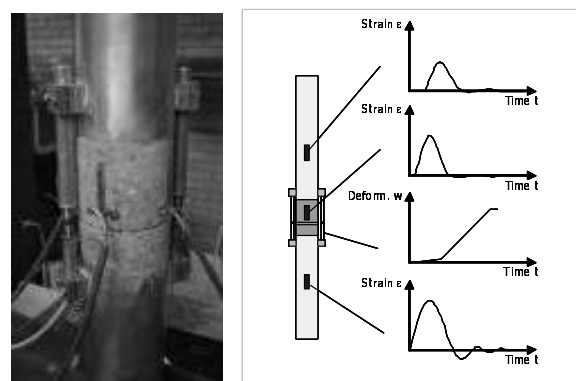


Figure 3. Instrumented notched specimen and scheme of SHB instrumentation.

4.3.2 Spalling technique, TNO-TU Delft

For the high loading rate regime (>1000 GPa/s), a Modified Split Hopkinson Bar (MSHB) set-up has been developed at TNO Defence, Security and Safety in Rijswijk. The feasibility of the set-up was demonstrated by the TNO prototype test set-up (Weerheijm et al 2004 and 2007). The MSHB is based on the principle of spalling. The MSHB set-up consists of a horizontal steel bar (length 2m, \varnothing 74mm), supported by strings (Figure 4). A compressive shock wave is introduced into the rod by detonating an explosive charge at one end of the bar. At the other end, a concrete specimen is attached. The specimen is first loaded in compression, but will fail in tension due to the reflected tensile wave (spalling).

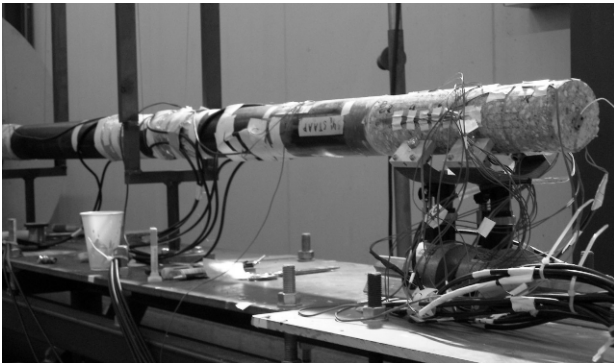


Figure 4. MSHB set-up with instrumented concrete specimen.

The measurement set-up of the MSHB is comparable to the set-up of the SHB, section 4.3.1. The transmitted pressure wave in the concrete specimen, the wave propagation and the reflection process are recorded with strain gauges distributed along the notched specimen (Figure 4-5). The loading rate and applied load are derived from the strain measurements on the steel bar and the specimen. The resulting stress at the failure zone (notch) is determined using the uniaxial wave theory. (Vegt, et al. 2007). To derive the desired stress-deformation curve, it is necessary to determine the deformation of the fracture zone directly.

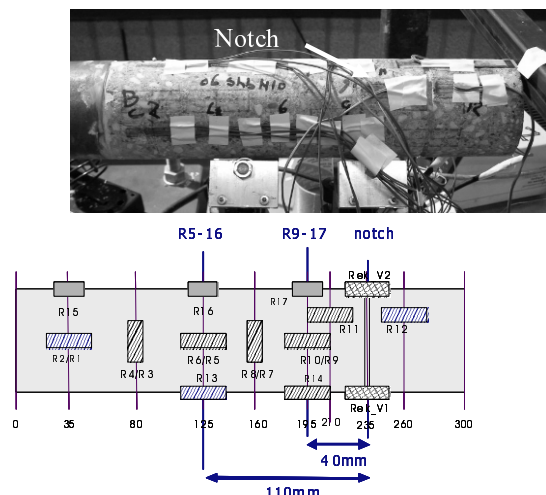


Figure 5. Instrumented concrete specimen.

New deformation gauges have been developed which are almost weightless and can measure deformations at very high loading rates. The measured deformations at the notch are combined with the resulting stresses in the notch to obtain the desired stress-deformation curve. This method is analogue to the method applied in statics and for the SHB in the moderate loading regime. Again, the area under this curve represents the fracture energy G_f . In Section 5 the results of static and dynamic tests are presented.

The diagnostic technique enables us to determine the fracture energy consistently with the methods applied in statics and the moderate loading regime. The dynamic Young's modulus and the induced loading pulse are also recorded. The strength can be determined and the failure process can be reconstructed. These are major advantages. The drawbacks are the scatter in the local measurements, which makes the analysis difficult and the uncertainty of the effect of structural inertia to the recorded stress-deformation curve. The latter aspect is currently studied in a computational project.

Alternative diagnostic and analysis techniques for spalling tests are presented in the next sections.

4.3.3 Spalling technique, EMI

At the Ernst Mach Institute in Germany, spall experiments are performed in a Hopkinson bar set-up without the transmitter bar. The loading pulse is generated by projectile impact. The concrete specimen itself is only instrumented with an accelerometer at the rear face to determine the dynamic strength (Curran et al. 2003). Notched and unnotched specimens are applied and the fracture process is recorded with high speed photography. Diagnostics and analysis are aiming at the average, global response and quantify the average response. The transmitted pressure pulse to the concrete specimen is derived from the recorded strain history at the incident bar (LE-wave theory). The dynamic Young's modulus in concrete follows from the same strain record and the arrival time of the pressure pulse at the rear face (accelerometer record). More interesting is the derivation of the fracture energy. No stress-deformation is obtained but the total fracture energy is derived from the impulse transfer during the spalling process that starts at t_1 and ends at t_2 (Schuler, et al. 2007). The stress distribution in the specimen is reconstructed assuming LE wave propagation without dispersion. Time t_1 is the moment that the dynamic strength is reached somewhere in the specimen. At that moment the spall process starts, the average velocities of the specimen parts at both sides of the fracture plane at t_1 are calculated. Both time t_2 when the crack is completely opened and the velocities of both specimen parts at t_2 , are obtained from the high speed recordings. Consequently the method relies on the sample frequency of the high speed recordings,

an objective criterion for “complete separation” and linear time dependency of the separation velocity and force during failure process. The fracture energy of the specimen is obtained from the change in momentum of the spall debris (ΔI_{spall}) and the mean crack opening velocity ($\dot{\delta}$) during the fracture process.

$$G_f = \Delta I_{spall} \cdot \dot{\delta}$$

The specific fracture energy is obtained by dividing this value by the fracture surface. Schuler proposes to derive the fracture surface from the ratio of the “accumulated crack length at the surface” and the circumferential length. Especially at high loading rates multiple fracture zones occur in unnotched specimen. Consequently these have to be distinguished to derive the G_f value for the single FZ (see discussion in 5).

The applied test method and diagnostics are relatively simple and straight forward. A draw back is the dependency of subjective criteria and visual interpretation of high speed recordings.

In section 5 the data obtained by Schuler and the authors will be compared and discussed.

4.3.4 Spalling technique, Metz University

Spalling tests on concrete are also performed at the Metz University. The set-up is similar to the EMI device. The main focus of the research is on the dynamic tensile strength, which is derived from the rear face velocity recorded optically using a laser. Recently, the shape of the impactor was modified and optimized to realize a “homogeneous stress distribution” for a large part of the specimen. (Erzar et al. 2009), which is a major advantage to obtain representative material strength data.

The focus of the current paper is on the fracture energy and therefore the previously reported results of Metz (Klepaczko and Brara 2007) have to be mentioned. In the 2007-paper, fracture energy data is presented that is derived from high speed recordings, stress distribution based on LE-wave theory and quite some assumptions on the fracture process. The mathematical approach is not very clearly presented. Because of these observations it is concluded by the authors that the results on fracture energy presented in (Brara et al. 2007) are questionable and unfortunately can not be used as reference data.

4.3.5 Dynamic Brazilian impact test

Another method presented in literature is the Brazilian splitting test in a Split Hopkinson Pressure bar set-up. Lambert and Ross (2000) tested specimen with a specially designed inner notch, to determine the rate effect on the fracture toughness of micro

concrete. The strain rate in the tests varied from $2/s - 8/s$, which corresponds to the regime of the SHB tests in Delft (section 4.3.1). The tests showed increase of K_{Ic} with a factor of 2, which is a considerable increase within the limited range of strain rates. The results indicate the rate dependency of the strength and fracture process for the tested concrete, but cannot be directly related to G_f . The theoretical relation of $G_f = K_{Ic}^2/E$ can not be used to quantify the rate effect because then it is implicitly assumed that the shape of the stress-deformation curve remains constant for all loading rates. Consequently, the rate dependencies of strength and fracture energy are assumed to be the same, which is in general incorrect.

Because this method does not directly provide data on the fracture energy and very specific specimen geometry is required, it is less suitable as a standard test than the 1D-Hopkinson set-ups.

5 DATA COMPARISON OF G_f -DATA FROM SPALLING TESTS

Reviewing the different test methods presented in literature, the 1D-Hopkinson bar set-up seems to be most suitable to quantify the dynamic strength as well as the dynamic fracture energy. The data analysis for these methods is also consistent with the static uniaxial tests, which is a major advantage to study and quantify the rate dependency. To illustrate the currently available data and need for bench mark activities, the available G_f -data for the high loading rate regime from EMI (Schuler 2006) and Delft are presented and discussed.

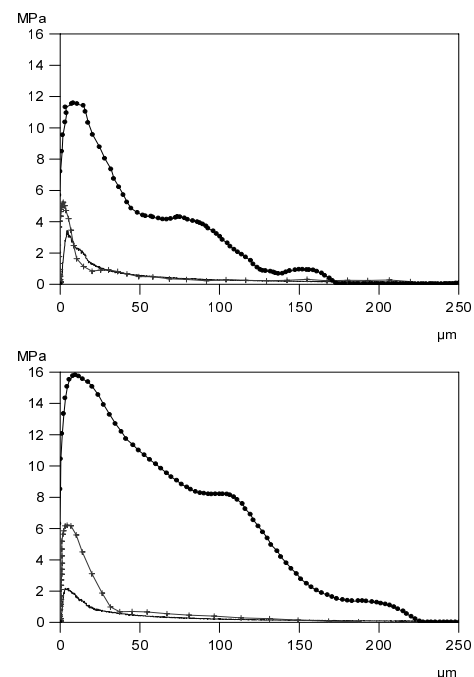


Figure 6. Stress–deformation curves for normal (top) and wet (bottom) condition.

The concrete specimens tested by EMI had a length of 250 mm and a diameter of 74.2 mm. The compressive cube strength f_c was 35 MPa, the static tensile strength f_t was 3.24 MPa and the Young's modulus $E_{stat} = 38.9$ GPa. The maximum aggregate size was 8 mm.

Details about the concrete tested at Delft are given in (Vegt 2007). The properties f_c , f_t and E_{stat} are respectively 48.2 Mpa, 3.4 Mpa and 35.1 GPa .

Note that the diameters of the specimen as well as the maximum aggregates size are the same for EMI and Delft.

In the Delft research program the dynamic strength and the load-deformation curves were derived for the reference concrete at normal, dry and wet conditions (see Vegt 2009). The stress deformation curves are given in Figure 6, the data in the Table Table 1. The data given by Schuler for normal conditions is summarized in Table 2.

Table 1. Strength, fracture energy and loading rate and dynamic/static ratios (Delft data).

	f_t	$/f_{t,Static}$	G_f	$/G_{f,Static}$	Loading rate
	MPa	-	N/m	-	GPa/s
<i>Normal</i>					
Static	3.30	1.0	120	1.0	$1 * 10^{-4}$
SHB	5.58	1.7	120	1.0	40
MSHB	10.3	3.1	728	6.1	1700
<i>Dry</i>					
Static	3.05	1.0	106	1.0	$1 * 10^{-4}$
SHB	4.73	1.6	139	1.3	40
MSHB	8.05	2.6	654	6.2	1700
<i>Wet</i>					
Static	2.05	1.0	80.3	1.0	$1 * 10^{-4}$
SHB	6.35	3.1	167	2.1	40
MSHB	15.8	7.7	1456	18.1	1700

Table 2. Strength, fracture energy and loading rate and dynamic/static ratios (EMI data).

	f_t	$/f_{t,Static}$	G_f	$/G_{f,Static}$	Loading rate
	MPa	-	N/m	-	GPa/s
<i>Normal</i>					
Static	3.24	1.0	125 [#]	1.0	$1 * 10^{-4}$
MSHB1*	12.9	4.0	289	2.3...	1300
MSHB2*	16.2	5.0	335	2.7	2600
MSHB3**	15.6	4.8	380	3.0	1150

Ad[#] Determined in 3 point bending test (RILEM)

Ad* Spalling test on un-notched specimen

Ad** Spalling test on notched specimen.

Comparing the MSHB-results for normal concrete, the observations and comments are:

- Concrete composition and static properties are not the same, but similar. Therefore, differences in observed rate effects are due to testing device, diagnostics and data analysis.
- Ratio of rate effect on f_t and G_f are: $4/2.3 = 1.7$ for EMI and $3.1/6.1 = 0.5$ for Delft. Because the ratio for EMI data is larger than 1, a more

brittle behavior is "observed" for these high loading rates. This is in contradiction with the data of Delft (for all moisture conditions) and the microscopic research of the fracture zone, see Figure 6 and Figure 7. A more ductile behavior and an increase in the amount of micro cracking and width of the fracture zone were observed.

- The width of the MSHB fracture zone is 25 mm for Delft. Using the EMI photograph of a crack pattern at the specimen surface, the width is in the same order (22 mm).

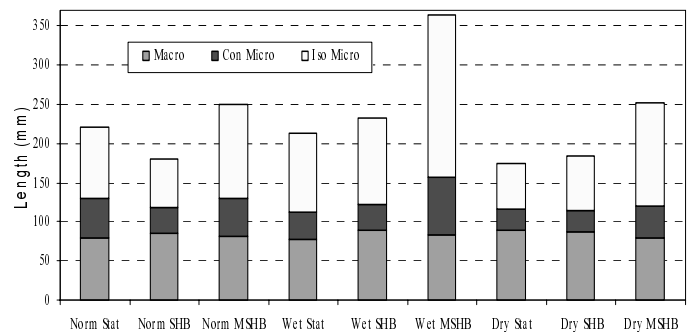


Figure 7. Width of fracture zone for all Delft test conditions.

To examine the consequences of assuming a linear time dependency of the separation velocities and force, the derived velocity-time curve in the Delft set-up is given in Figure 8. The maximum velocity of 2.5 m/s corresponds to the "EMI-velocity" of 2-2.6 m/s. From the displacement recordings it was concluded that the failure process occurs between $t = 465-500$ μsec . Note this time is much longer than the "8 μsec " estimated for the bridging time between dominant defects (section 4.1). Calculating G_f according to

$$G_f = \int_{t_{frac}} F(t) \cdot \dot{\delta}(t) \cdot dt$$

a linear time dependency of the separation velocity and softening force will lead to an underestimation of G_f .

Combining these observations, the preliminary conclusion is that the data analysis and optical observations at EMI probably result in an underestimation of the fracture energy. The conclusion is preliminary because the data comparison is very limited and the Delft data most probably overestimates G_f because of the structural response effects in the deformation recordings resulting in the "bulges" in the softening branch (Figure 6).

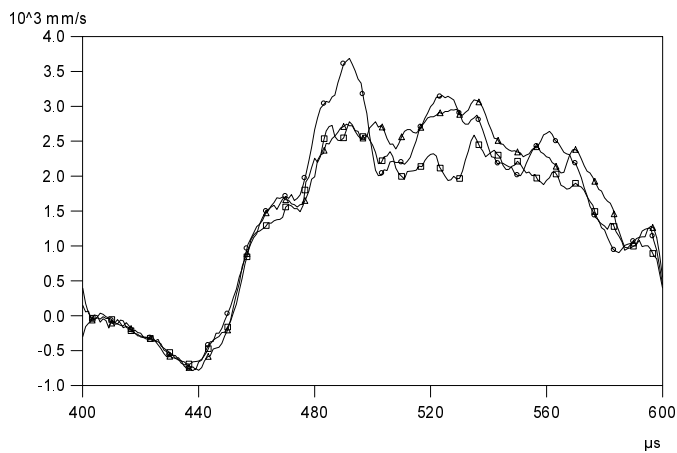


Figure 8. Separation velocity-time curve in Delft set-up.

The data comparison presented, illustrates the need of international cooperation, benchmarking and standardization in order to compare dynamic test data. Referring to the long, but also inspiring research and development episode of the RILEM test, a trilateral cooperation between Metz, EMI and Delft would be a good start.

6 CONCLUSIONS AND RECOMMENDATIONS

Data on the dynamic fracture energy of concrete are scarce and also not consistent due to different test methods, data analysis and definitions. This paper intends to facilitate the discussion and the standardization process of dynamic tensile tests.

Test methods to derive strength and, especially fracture energy data for concrete in tension are summarized and reviewed. Definitions of the fracture process zone, the fracture zone and the fracture energy are recalled.

It is concluded that for dynamics the uniaxial set-ups are the most suitable because the stress distribution as a function of time can be recorded or (easily) derived for the specimen and the fracture zone. It is strongly recommended to invest in measurement techniques to measure the deformation of the fracture zone directly.

With reference to the sections 4.3 and 5, the recommended test methods and specimen geometries for dynamic tensile testing are:

- Split Hopkinson tension bars for the loading rate regime in the order of $\dot{\sigma} = 10 - 100$ GPa/s (order $\dot{\epsilon} \approx 1 - 10$ 1/s).
 - Strength $f_{t,dyn}$: un-notched specimen (preferred)
 - Fracture energy $G_{f,dyn}$: notched specimen
 Note that strength data can also be obtained from notched experiments.
- Hopkinson Spalling technique for loading rates beyond 100 GPa/s.
 - Strength $f_{t,dyn}$: specimen unnotched and velocity recording by laser. (preferred)

- Strength $f_{t,dyn}$ (alternative): notched specimen
- Fracture energy $G_{f,dyn}$: notched specimen and diagnostics to record stress conditions and deformation in notched area directly.

International cooperation and a benchmark program on dynamic tensile testing are recommended. A direct comparison of data and exchange of information can lead to standardization in dynamic testing and will enable the comparison of dynamic test data.

REFERENCES

- Bazant, Z.P. and Oh, B.H. 1983. Crack band theory for fracture of concrete. RILEM Materials and Structures, 16 (93), pp 155-177.
- Carpinteri, A. 1984. Stability of fracture process in RC beams. J. Structural engineering, 110, pp 2073-2084.
- Curran, D.R, Kanel, G.I., Razorenov, S.V. Utkin, A.V. 2003. Spall fracture. ISBN 0-387-95500-3. Springer Verlag.
- Duan, K., Hu, X. and Wittman, F.H. 2007. Size effect on specific fracture energy of concrete. Engineering Fracture Mechanics 74. pp. 87-96.
- Erzar, B. and Forquin, F. 2009. An Experimental Method to Determine the Tensile Strength of Concrete at High Rates of Strain. Experimental Mechanics, accepted August 2009
- Elices, M., Guinea, G.V., Planas, J. 1992. Measurement of the fracture energy using 3-point bend tests. 3. Influence of cutting the p-delta tail. Materials and Structures. 1992; 25: 327-35.
- Elices, M., Guinea, G.V., Planas, J. 1997. On the measurement of the fracture energy using 3-point bend tests. Materials and Structures. 1997; 30: 375-6
- Guinea, G.V., Planas, J., Elices, M. 1992. Measurement of the fracture energy using 3-point bend tests. 1. Influence of experimental procedures. Materials and Structures. 1992; 25:212-8
- Hillerborg, A. Modeer, M and Petersson, P.E. 1976. Analysis of crack formation and crack growth in concrete by means of fracture mechanics and finite elements. Cement and Concrete Res., 6, pp 773-782.
- Hillerborg, A. 1985. The theoretical basis of a method to determine the fracture energy G_f of concrete. RILEM Materials and Structures, 18 (106), pp 291-296.
- Mier, J.G.M. 1996. Fracture processes of Concrete: assessment of material parameters for fracture models. CRC Press.
- Mier, J.G.M. van, Vliet, M.R.A. van. 2002. Uniaxial tension test for the determination of fracture parameters of concrete: state of the art. Engineering Fracture Mechanics 69, pp. 235-247.
- Planas, J., Elices, M., Guinea, G.V. 1992. Measurement of the fracture energy using 3-point bend tests. 2. Influence of bulk energy dissipation. Materials and Structures. 1992; 25: 305-12.
- Schuler, H., Mayrhofer, C. and Thoma, K. 2006. Spall experiments for the measurement of the tensile strength and fracture energy of concrete at high strain rates. Int. J. of Impact Engineering 32, 1635-1650.
- Reinhardt, H.W. 1984. Fracture mechanics of an elastic softening material like concrete. HERON, 29 (2), 42 pp.
- Vegt, I., Weerheijm, J. and Van Breugel, K. 2007. The fracture energy of concrete under impact tensile loading- a new experimental technique. CONSEC Conference June 2007, Tours, France.

- Vegt, I. Breugel, K. van and Weerheijm, J. 2007. Failure mechanisms of concrete under impact loading. FraMCoS-6, Catania, Italy, 17-22 June 2007.
- Weerheijm, J. and van Doormaal, J.C.A.M. ,2007. "Tensile failure of concrete at high loading rates: New test data on strength and fracture energy from instrumented spalling tests. Int. J. of Impact Engineering 34 (2007), pp 609-626.
- Weerheijm, J. and van Doormaal J.C.A.M. 2004. Tensile failure at high loading rates; Instrumented spalling tests. International Conference FramCoS 5, April 200
- Zhang, X.X., Ruiz, G., Yu, R.C. and Tarifa, M. 2009. Fracture behaviour of high-strength concrete at a wide range of loading rates. Int. J. of Impact Engineering, 36, pp 1204-1209.